Zhang et al. *Zool. Res.* 2026, 47(3): 988−1002
https://doi.org/10.24272/j.issn.2095-8137.2025.170
https://cstr.cn/32248.14.zr.2025.170

ZR | Zoological Research

Article Open Access

A secretion-deficient DENV1 DNA vaccine induces durable immunity and confers protection against DENV2

Chen Zhang[1,2,#], Kai-Hao Feng[3,#], Yu-Xuan Liu[1,2], Chong-Yao Zhong[1,2], Kun-Qi Lin[1,2], Hui Chen[1], Dong-Ying Fan[1,2], Jing An[1,2,*], Pei-Gang Wang[1,2,*], Na Gao[1,2,*]

[1] *Department of Microbiology*, *School of Basic Medical Sciences*, *Capital Medical University*, *Beijing* 100069, *China*

[2] *Laboratory for Clinical Medicine*, *Capital Medical University*, *Beijing* 100069, *China*

[3] *Graduate School*, *Peking Union Medical College*, *Chinese Academy of Medical Sciences*, *Beijing* 100005, *China*

ABSTRACT

Antibody-dependent enhancement (ADE) remains a major obstacle to dengue virus (DENV) vaccine development and continues to make safe, broadly protective vaccination a global health priority (Aggarwal et al., 2024; Halstead et al., 2014; Martinez et al., 2021; Paz-Bailey et al., 2024; Shepard et al., 2016). This study generated two DNA-based DENV vaccine constructs encoding premembrane (prM) and envelope (E) proteins: a secretion-deficient mutant (DNSP) and a full-length wild-type (WT) prM-E protein. Both vaccines elicited cell-mediated immune responses and protected mice against lethal DENV1 challenge. DNSP immunization induced minimal anti-prM-E antibody production but conferred durable protection, as evidenced by sustained T cell responses and challenge experiments performed one year after vaccination. *In vitro* DENV infection assays further showed that DNSP reduced K562 cell infection across all four DENV serotypes. *In vivo* DENV2 challenge also demonstrated that DNSP conferred effective protection against DENV2 infection. These findings identify secretion-deficient prM-E DNA vaccination as a promising strategy for strengthening cell-mediated antiviral immunity while limiting antibody induction. DNSP may therefore serve as a booster immunogen with potential to reduce ADE-associated risk during DENV vaccination.

Keywords: DNA vaccine; Dengue virus; Antibody-dependent enhancement (ADE)

INTRODUCTION

Since the first isolation of dengue virus (DENV) in 1943, four antigenically distinct serotypes have been identified. Over subsequent decades, dengue epidemics have expanded across tropical and subtropical regions, from Asia to the Americas, creating a persistent and escalating public health burden. Current estimates indicate that approximately 390 million infections occur annually, including around 96 million clinically apparent cases (Bhatt et al., 2013; Guo et al., 2017; Kayesh et al., 2023). Large-scale dengue outbreaks have affected numerous countries in recent years. The World Health Organization (WHO) reported more than 3.5 million dengue cases in the Americas in the first three months of 2024, representing a three-fold increase compared with the same period in 2023, itself a record-breaking year (Tian et al., 2022). In China, substantial dengue outbreaks have been reported across multiple provinces and cities, with over 19 000 cases documented in 2024, highlighting the continuing threat posed by dengue fever (Lee et al., 2024; Sahak, 2020; Yue et al., 2022). Infected individuals typically develop self-limiting disease characterized by fever, rash, and systemic discomfort. However, severe cases can progress to dengue hemorrhagic fever (DHF) or dengue shock syndrome (DSS), with clinical manifestations that include abdominal pain, vomiting, nasal bleeding, thrombocytopenia, and hepatomegaly (Copaja-Corzo et al., 2024; Vuong et al., 2024).

DENV is an enveloped, positive-sense RNA virus with an approximately 10.7 kb genome translated into a single polyprotein, which is subsequently processed into three structural proteins (capsid (C), premembrane (prM), and envelope (E)) and seven non-structural proteins (NS1, NS2A, NS2B, NS3, NS4A, NS4B, and NS5). Virion assembly occurs in the lumen of the endoplasmic reticulum (ER), where immature particles form through the organization of 60 prM-E heterotrimers. The E protein ectodomain contains three domains, DI, DII, and DIII, and constitutes the principal target of most neutralizing antibodies and vaccines(Tan et al., 2020).

During passage through the acidic Golgi network, furin-

Received: 22 October 2025; Accepted: 09 December 2025; Online: 10 December 2025

Foundation items: This work was supported by the National Key Research and Development Plan of China (2021YFC2300202 to J.A.), Natural Science Foundation of Beijing (QY24340 to K.Q.L.), Natural Science Foundation of Beijing (7232002 to N.G.), and National Natural Science Foundation of China (82241071 to J.A.; 82372251, 81871641, and 82172266 to P.G.W.)

[#]Authors contributed equally to this work

*Corresponding authors, E-mail: gao_na@ccmu.edu.cn; pgwang@ccmu.edu.cn; anjing@ccmu.edu.cn

mediated cleavage of prM enables release of the pr peptide in the extracellular space, thereby generating mature infectious particles. However, the extent to which intracellular host receptors regulate trafficking and secretion of progeny virions remains unclear. Previous research has demonstrated that DENV interacts with KDEL receptors (KDELRs), host retrieval proteins that shuttle between the ER and Golgi apparatus and facilitate vesicular transport of newly formed viral particles. KDELR depletion by siRNA reduces the release of both DENV progeny and recombinant subviral particles (RSPs). Further analysis identified amino acids at positions 2, 19, and 21 of prM as key residues required for KDELR binding. Substitution of these three amino acids allows intracellular production of DENV subviral particles but prevents their release into the extracellular space, thereby generating secretion-deficient DENV subviral particles (Li et al., 2015).

Secretion-deficient viral particles provide a rational approach for redirecting vaccine-induced immunity. Because these particles are retained intracellularly, they may undergo proteasomal degradation and generate endogenous antigenic peptides for major histocompatibility complex class I (MHC-I) presentation, thereby promoting cytotoxic T lymphocyte (CTL) activation. In contrast, reduced extracellular release is expected to limit uptake by antigen-presenting cells (APCs) through phagocytosis or endocytosis, decrease MHC-II-mediated antigen presentation, and attenuate humoral responses.. This immunological profile is particularly relevant to DENV vaccine development because antibody-dependent enhancement (ADE) remains a central safety concern. Strong or imbalanced antibody responses, especially non-neutralizing antibodies, can lead to ADE and worsen disease symptoms. The DNSP vaccine may therefore reduce ADE risk by decreasing humoral immunity while strengthening cellular immunity required for clearance of infected cells (Biswal et al., 2020; Guirakhoo et al., 2001; Kariyawasam et al., 2023; Santos-Peral et al., 2024; Thomas & Yoon, 2019).

This study developed two DNA vaccine constructs encoding the full-length DENV prM and E proteins: a secretion-deficient mutant (DNSP) and a wild-type (WT) construct. Both vaccines were immunogenic and protected mice in a lethal DENV challenge model, but DNSP induced markedly lower antibody levels. After three immunizations, DNSP elicited strong T cell responses comparable to those induced by WT vaccination and reduced ADE-associated infection across all four DENV serotypes in K562 cells. In A6 mouse models of DENV2 infection, DNSP conferred effective protection against viral challenge. Together, these findings indicate that secretion-deficient prM-E expression can preserve durable protective immunity while limiting antibody induction and reducing ADE-associated infection in vitro, supporting DNSP as a promising direction for safer DENV vaccine development.

MATERIALS AND METHODS

Experimental animals

Six-week-old BALB/c mice were purchased from Beijing Vital River Laboratory Animal Technology Co., Ltd. (China). A6 mice lacking the IFN-α/β receptor were provided by the Institute of Laboratory Animal Science, Peking Union Medical College (China). All mice were bred, maintained, and handled under specific pathogen-free (SPF) conditions in the animal facility at Capital Medical University.

Ethics statement

All animal experiments and protocols were approved by the Animal Welfare and Ethics Committee of Capital Medical University (Approval No. AEEI-2024-140). All efforts were made to minimize the number of animals used, and experimental design was optimized to maximize information obtained from each animal in accordance with ethical guidelines.

Viruses

The DENV1, DENV2, DENV3, and DENV4 strains used in this study were Hawaii (GenBank: EU848545), Tr751 (GenBank: KF752596.1), H87 (GenBank: M93130), and H241 (GenBank: AY947539), respectively. DENV was propagated in C6/36 cells. Viral titers were determined by plaque assay on Vero cells under 1.2% methylcellulose overlay medium. Concentrated DENV protein was prepared from the supernatant of DENV-infected C6/36 cells containing 8% polyethylene glycol.

Immunohistochemical staining

Thigh muscles and spleens were collected 3 weeks after the final immunization. Paraffin-embedded sections were processed using established techniques, as described previously [63]. Rabbit anti-CD4 (ab183685, Abcam, USA) and rabbit anti-CD8a (ab199016, Abcam, USA) antibodies were obtained for use, while mouse anti-4G2 antibodies were prepared and stored in the laboratory. Primary antibodies were diluted 1:500. Horseradish peroxidase (HRP)-conjugated goat anti-mouse IgG (Santa Cruz Biotechnology, USA) and HRP-conjugated goat anti-rabbit IgG (Santa Cruz Biotechnology, USA) were each diluted 1:2,000 and used as secondary antibodies.

Enzyme-linked immunosorbent assay (ELISA)

DENV1-specific total IgG antibodies in mouse serum were measured by ELISA using a commercial DENV1-IgG kit (Saipuson Biotechnology, China). Color intensity was positively associated with DENV-specific IgG antibody (DF-IgG) concentration. Absorbance was measured at 450 nm, and antibody concentrations were calculated according to the kit instructions.

Plaque reduction neutralization test

DENV-specific neutralizing antibodies were quantified using a plaque reduction neutralization test (PRNT). Heat-inactivated serum samples were serially diluted 2-fold from 1:10 to 1:1 280 with Minimum Essential Medium (MEM) containing 2% fetal bovine serum (FBS). Diluted serum samples were mixed with an equal volume of viral solution containing 100 plaque-forming units (PFU) of DENV and incubated for 1 h at 37°C. The mixtures were then added to Vero cells and incubated for 1 h at 37°C. Cells were cultured under overlay medium, and plaques were visualized by crystal violet staining. The 50% and 80% neutralizing titers ($PRNT_{50}$ and $PRNT_{80}$) were defined as the reciprocal of the highest serum dilution that reduced the mean plaque number by 50% or 80%, respectively, relative to virus control wells containing normal mouse serum. In this study, $PRNT_{50}$>1:10 was defined as the cutoff for neutralizing antibody positivity.

Cytokine profile assay

Cytokine secretion by splenocytes was analyzed by ELISPOT according to the recommendations from the manufacturer (BD, USA). In brief, 96-well filtration plates (Millipore, USA) were coated with capture antibodies at 4°C overnight and blocked with 1% bovine serum albumin (BSA) at 37°C for 2 h. Splenocytes isolated from immunized mice were aliquoted at

5×10^5 cells/well and stimulated with purified DENV1 particles at 5 μg/well at 37°C for 48 h. After incubation with biotinylated detection antibody, spots were developed using streptavidin-HRP and 3-amino-9-ethylcarbazole (AEC) substrate and quantified automatically with an ELISPOT analyzer (CTL, USA). Splenocytes cocultured with concanavalin A served as positive controls, whereas splenocytes cultured with RPMI 1640 medium served as negative controls.

Flow cytometry analysis

All antibodies used for flow cytometry were purchased from BD Biosciences (USA). A total of 2×10^6 splenic lymphocytes were blocked with rat anti-mouse CD16/CD32 monoclonal antibody for 30 min. For surface staining, cells were incubated with anti-CD3e-FITC, anti-CD8-APC-H7, anti-CD44-APC, and anti-CD62L-PE at standard dilutions. Stained cells were acquired on a DxFLEX flow cytometer (Beckman Coulter, USA) and data were analyzed using CytExpert software (v1.2).

ADE experiment *in vitro*

Serum collected from mice immunized 1 year earlier was heated at 56°C for 30 min to inactivate complement and then serially diluted from 1:10 to 1:10 000. Groups included 4G2-positive controls, virus-only infected K562 cells, and uninfected cell-only controls. Diluted serum was mixed with DENV and incubated for 30 min at 37°C in a 5% CO_2 incubator to allow virus-antibody complex formation. K562 cells were then added to the virus-serum mixtures and incubated for 1–2 h at 37°C in a 5% CO_2 incubator to permit infection. After washing, cells were maintained for an additional 48 h under the same culture conditions. Cells were collected, washed, fixed with 4% paraformaldehyde (PFA), permeabilized, and blocked with 1% BSA. Cells were incubated with primary antibody (4G2) at 4°C for 45–60 min, washed, and incubated with secondary antibody (goat anti-mouse IgG-488) at 4°C for 45 min in the dark. After final washing, cells were analyzed by flow cytometry. ADE positivity was defined using the mean number of positive cells in the virus-only infected K562 cell group plus three standard deviations (SDs) as the baseline threshold. Values above this threshold were considered ADE positive, while those below were considered negative.

ADE experiment *in vivo*

Immune serum was heat-inactivated at 56°C for 30 min and then incubated with DENV2 at room temperature for 1 h. Each A6 mouse received an intraperitoneal injection of 300 μL of the virus-serum mixture, consisting of 200 μL of viral solution and 100 μL of immune serum. Body weight was recorded daily, and clinical signs were monitored throughout the observation period.

Viral load detection

Total RNA was extracted from whole blood and tissue samples using TansZol reagent. Viral RNA loads were quantified by real-time reverse transcription polymerase chain reaction (RT-qPCR). using a commercial reagent kit. Each 20 μL reaction mixture was prepared following the manufacturer's protocols, and amplification was performed on the ABI 7500 real-time PCR platform. A standard curve was generated by plotting the logarithm of viral copy number against the corresponding Ct value. Viral load was calculated from the regression equation and expressed as DENV2 copy number per μg of total RNA. Primers used were Forward: 5'-CATGGGTAACTTATGGGAC-3' and Reverse: 5'-GTTTCAGT TCGTGTCTCCA-3'.

Cytotoxic T lymphocyte activity

Two weeks after vaccination, freshly isolated mouse splenocytes were stimulated with concentrated DENV1 proteins (2 μg/10^5 cells) for 72 h to generate effector cells. L929 cells infected with DENV1 at a multiplicity of infection (MOI) of 10 for 16–18 h served as target cells. Target cells were seeded in U-bottom 96-well plates at 5×10^3 cells/well and cultured with effector cells at effector-to-target (E:T) ratios of 100:1, 50:1, 20:1, and 10:1. After incubation for 5 h at 37°C and 5% CO_2, 50 μL of supernatant from each well was transferred to 96-well flat-bottom plates. Lactate dehydrogenase (LDH) activity was quantified using the CytoTox nonradioactive cytotoxicity assay kit (Promega, USA) per the manufacturer's instructions. Absorbance was measured at 490 nm with a microplate reader. Specific cytotoxicity was calculated as follows: % cytotoxicity= 100×(experimental release−effector spontaneous release−target spontaneous release)/(target maximum release−target spontaneous release).

Western blotting

Supernatants from Vero cells transfected with plasmids were harvested and lysed in radioimmunoprecipitation assay (RIPA) buffer containing protease inhibitor. Protein concentration was determined using a BCA Protein Assay kit. Equal amounts of protein were separated by 10% sodium dodecyl sulfate-polyacrylamide gel electrophoresis (SDS-PAGE) and transferred onto polyvinylidene difluoride (PVDF) membranes. After blocking with 5% milk at room temperature for 1 h, membranes were incubated with 4G2 antibody at 4°C overnight and then with goat anti-mouse secondary antibody. Protein bands were visualized using an Odyssey infrared imaging system (Odyssey LI-COR Biosciences, USA).

Statistical analysis

Data were analyzed using GraphPad Prism v8.0.1. Normally distributed data were compared using Student's t-test for two-group comparisons or analysis of variance (ANOVA) for multiple-group comparisons, as appropriate. All results are presented as mean±standard error of the mean (SEM) from at least three independent experiments. Survival rates were compared using the log-rank test. $P<0.05$ was considered statistically significant.

RESULTS

pVAX1-DNSP and pVAX1-WT induce distinct antibody responses

Three DNA plasmids were generated for immunogenicity assessment: pVAX1-control, which contained no transgene; pVAX1-WT, which encoded full-length DENV1 prM-E; and pVAX1-DNSP, which encoded DENV1 prM-E containing three amino acid substitutions designed to impair secretion. Each target gene was inserted under transcriptional control of the T7 promoter. Full-length prM-E was expected to assemble into secreted virus-like particles (VLPs), whereas the secretion-deficient prM-E mutant was designed to form VLPs that failed to undergo extracellular secretion (Figure 1A). The production of DENV E protein in the Vero cells infected with WT but not DNSP was confirmed by immunofluorescence assays (IFA). Experimental results (Figure 1B) showed that both the WT and DNSP dengue DNA vaccines successfully induced E protein expression within cells 24 hours post-transfection. We

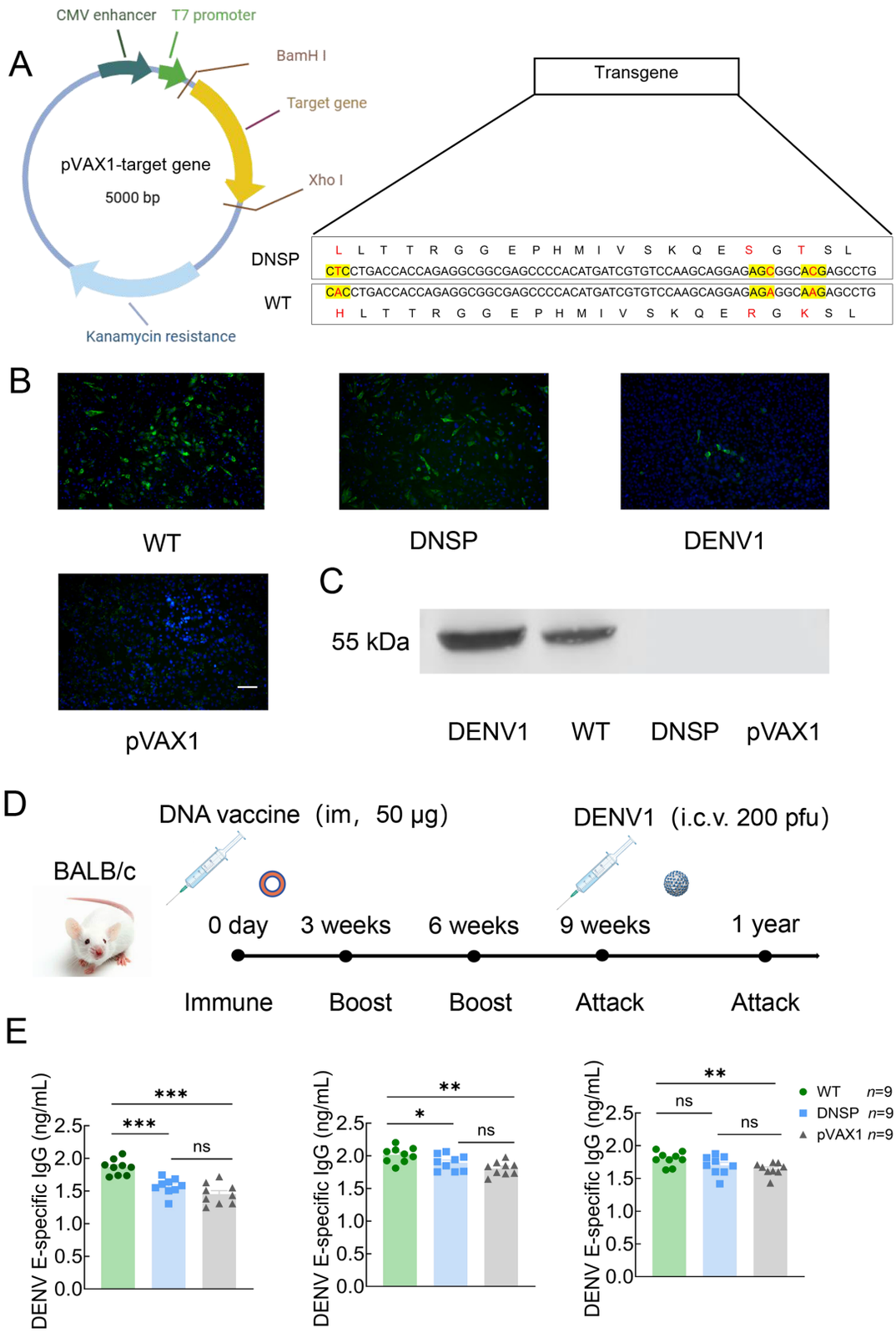

Figure 1 Immunogenicity of pVAX1-DENV1 vaccines in BALB/c mice

A: Plasmid design. The pVAX1 control vector contained no transgene insert, whereas DNSP and WT encoded secretion-deficient DENV1 prM-E or full-length prM-E, respectively. B: DENV E protein expression in Vero cells. Vero cells were transfected with DNSP, WT, or pVAX1, and E protein expression was detected by immunofluorescence staining using the 4G2 antibody. Scale bar, 200 μm. C: DENV E protein expression in transfected-cell supernatants. Vero cells were transfected with DNSP, WT, or pVAX1, and E protein (55 kDa) in culture supernatants was detected by western blotting. D: Immunization schedule in BALB/c mice. Mice received 50 μg of pVAX1, WT, or DNSP DNA plasmid via intramuscular electroporation, followed by booster immunizations at 3 and 6 weeks. E: Humoral immune responses. Serum E-specific IgG levels were measured by ELISA at 21 days post-primary immunization, 21 days post-booster, and 365 days post-booster. Data are presented as mean for each group (n=9). Data were analyzed by Student's t-test. ns: Not significant; *: P<0.05; **: P<0.01; ***: P<0.001; ****: P<0.0001. CMV: Cytomegalovirus, WT: Wild-type, DNSP: Dengue non-secreting particle.

detected the content of E protein in the transfected supernatant by Western blot method. The experimental results showed that no E protein was detected in the supernatant after DNSP plasmid was transfected (Figure 1C).

The immunogenicity of pVAX1-WT and pVAX1-DNSP was then examined in immunocompetent BALB/c mice. Eight-week-old mice received 50 μg of each DNA construct via intramuscular injection followed by electroporation. Booster immunizations with the same construct were administered 3 and 6 weeks after the primary dose. Serum samples were collected at 3 weeks post-primary immunization, 3 weeks post-booster immunization, and 1 year after the final booster (Figure 1D). DENV E protein-based ELISA showed that pVAX1-WT induced higher DENV-specific IgG levels than pVAX1-DNSP and pVAX1-control after primary immunization, with mean concentrations of 1.862±0.040, 1.570±0.042, and 1.452±0.053 ng/mL, respectively (Figure 1E). The third vaccine dose slightly increased DENV-specific IgG levels in all groups, with mean concentrations of 2.015±0.039, 1.894±0.040, and 1.807±0.034 ng/mL, respectively. At 1 year post-immunization, pVAX1-WT maintained significantly higher DENV-specific IgG levels than pVAX1-DNSP and pVAX1-control, with mean concentrations of 1.798±0.036, 1.699±0.048, and 1.643±0.032 ng/mL, respectively.

Neutralizing antibody responses were further quantified by PRNT. At 3 weeks after primary immunization, pVAX1-WT induced higher neutralizing activity against DENV than pVAX1-DNSP, with $PRNT_{50}$ values of 33.125±9.608 and 10.625±1.943, respectively. Neutralizing antibody levels increased after the third immunization, reaching $PRNT_{50}$ values of 145.000±37.081 for pVAX1-WT and 28.125±8.372 for pVAX1-DNSP. One year after the final immunization, neutralizing antibody levels did not differ significantly between the pVAX1-DNSP and pVAX1-control groups (Figure 2A–C).

Cross-neutralizing activity against heterologous DENV serotypes was also assessed by PRNT using serum collected 1 year after immunization. pVAX1-WT induced higher cross-neutralizing antibody titers against DENV2 than pVAX1-DNSP, with $PRNT_{50}$ values of 26.25±4.912 and 11.25±1.816, respectively. In contrast, pVAX1-DNSP induced little to no detectable cross-neutralizing activity against DENV3 or DENV4 (Figure 2D–F).

Vaccine-induced T cell immune responses against DENV

To determine whether the two vaccine constructs elicited $CD8^+$ T cell responses, mice were immunized and boosted as described above, and muscle tissue from the injection site and spleens were collected 3 weeks after the final immunization. Immunohistochemical staining of splenic germinal centers showed that $CD4^+$ T cells in the DNSP group were more diffusely distributed and were significantly reduced within germinal centers compared with the WT group (148.066±66.413 vs. 233.798±44.082), with an apparent shift toward the germinal center periphery. $CD8^+$ T cells in the DNSP group showed a more compact distribution pattern, with fewer cells than in the WT group and a greater proportion localized outside germinal centers (Figure 3A–C). T cell responses at the injection site also differed between vaccine groups: DNSP showed stronger local E protein expression in muscle tissue and tended to induce higher numbers of $CD4^+$ and $CD8^+$ T cells than WT ($CD4^+$: 0.642±0.185 vs. 0.235±0.123; $CD8^+$: 0.699±0.25vs. 0.217±0.114) (Figure 3D–F).

DENV-specific memory T cell responses were further examined in the spleen. After restimulation with DENV viral particles, splenic $CD8^+$ T cells were stained and analyzed by flow cytometry. Central memory T cells ($CD44^{High}CD62L^{High}$) were detected in the WT (8.2%±1.522%), DNSP (12.49%±1.037%), and pVAX1 control (2.76%±1.423%) groups (Figure 4A–C). Cytokine release after stimulation with DENV viral particles was then quantified by ELISPOT. The mean numbers of IL-2, IL-4, IFN-γ, and TNF spots in the pVAX1-DNSP group were 63, 676.125, 230.25, and 679 SFU/5×10^5 splenocytes, respectively. The corresponding values were 80, 716.25, 262.25, and 575 SFU/5×10^5 splenocytes in the WT group and 44.875, 58.75, 36.625, and 124.75 SFU/5×10^5 splenocytes in the pVAX1 group, respectively. DNSP therefore induced markedly higher secretion of Th1-associated cytokines, including TNF and IFN-γ, as well as the Th2-associated cytokine IL-4, than the control vector. These findings suggest that DNSP can induce antigen-responsive cellular immunity and promote a cytokine profile compatible with protective T cell responses against DENV1 (Figure 4D).

Vaccine-induced cytotoxic T lymphocyte (CTL) effector function was then evaluated by measuring antigen-specific cytotoxicity in immunized mouse splenocytes. As shown in Supplementary Figure S1, CTL activity was significantly higher in both the WT and DNSP groups than in the pVAX1 group across all E:T ratios ($P<0.05$), with a dose-dependent increase at higher ratios (e.g., 10:1: WT 5.0%, DNSP 5.9%, pVAX1 2.0%; 100:1: WT 14.2%, DNSP 15.1%, pVAX1 7.9%). CTL responses induced by DNSP and WT did not differ significantly at any tested E:T ratio.

pVAX1-DNSP reduces heterotypic DENV-mediated ADE in K562 cells

To determine whether pVAX1-DNSP altered heterotypic DENV enhancement risk, *in vitro* ADE assays were performed using FcγR-expressing K562 cells. Serum collected from mice 1 year after the final immunization was serially diluted, incubated with DENV, and then added to 10 000 K562 cells. The proportion of infected cells was then quantified by flow cytometry. The ADE detection threshold was defined as the mean positive-cell ratio in K562 cells infected with virus alone plus three SDs. Infection rates across four serum dilutions (1:10, 1:100, 1:1 000, 1:10 000) were plotted, and the area under the curve (AUC) above the detection baseline was calculated. The AUC value from the pVAX1-control group was used as the reference baseline for comparison.

For DENV1, the AUC in the pVAX1-DNSP group (3.59±0.238) was significantly lower than those in the pVAX1-WT (5.55±0.449) and pVAX1-control (7.366±0.378) groups. For heterotypic serotypes, no significant differences were detected between pVAX1-DNSP and pVAX1-control for DENV2 (pVAX1-DNSP, 9.846±0.531; pVAX1-WT, 11.534±0.420; pVAX1-control, 9.017±0.413), DENV3 (pVAX1-DNSP, 4.929±0.278; pVAX1-WT, 6.439±0.389; pVAX1-control, 5.521±0.409), or DENV4 (pVAX1-DNSP, 4.259±0.278; pVAX1-WT, 5.059±0.283; pVAX1-control, 4.004±0.163) (Figure 5). The data indicate that pVAX1-DNSP conferred a lower cellular ADE profile that pVAX1-WT. Consistently, serum from pVAX1-DNSP-vaccinated mice maintained infection rates comparable to those observed in the pVAX1-control group across the dilution series for DENV2, DENV3, and DENV4 (Supplementary Figure S2).

pVAX1-DNSP and pVAX1-WT protect mice against lethal DENV1 challenge

Immunocompetent BALB/c mice were immunized with pVAX1-

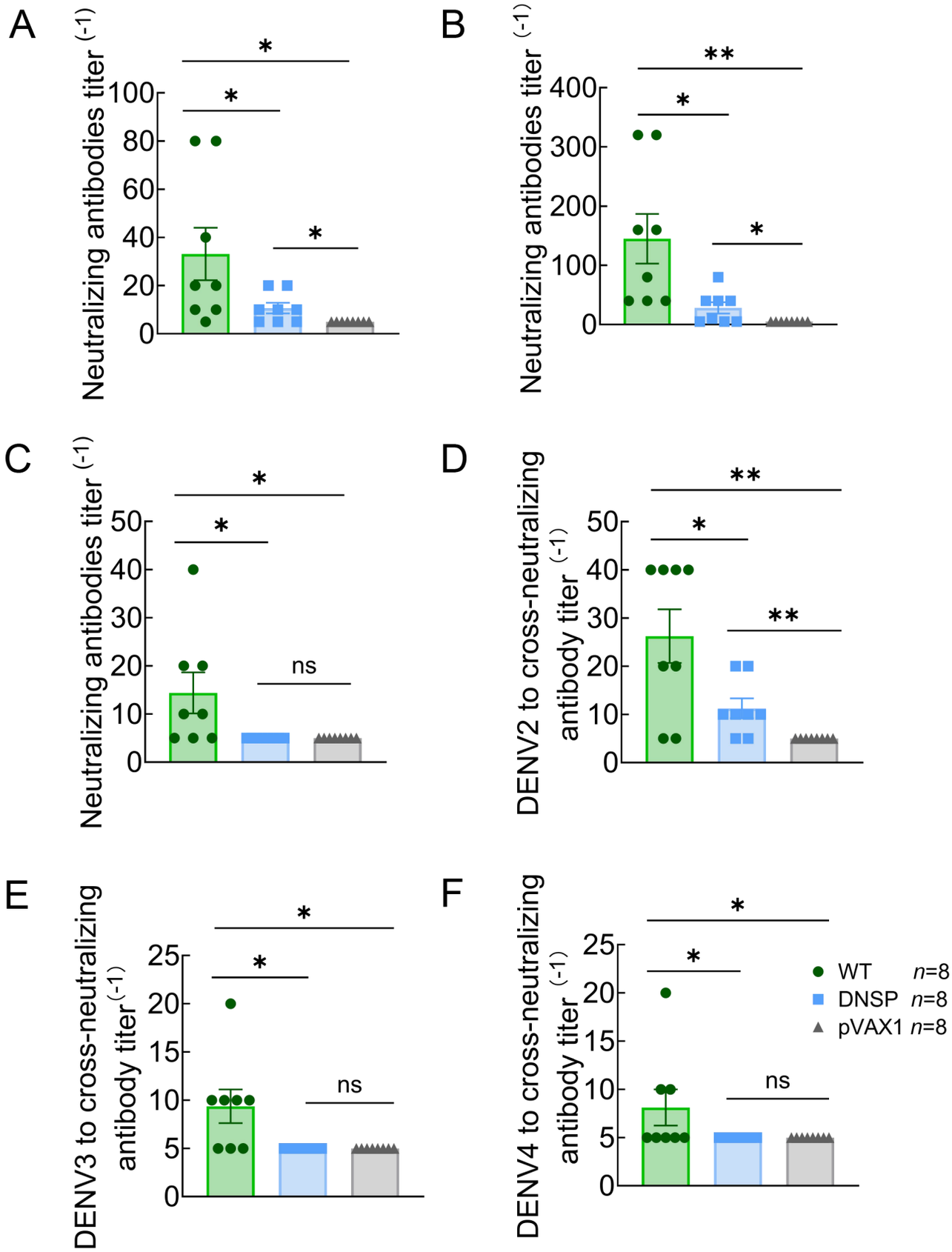

Figure 2 Neutralizing antibody production and cross-serotype reactivity induced by pVAX1-DENV1 DNA vaccination

Six-week-old BALB/c mice were immunized with 50 μg of pVAX1, WT, or DNSP DNA plasmid and received homologous booster doses at weeks 3 and 6 after primary immunization (n=8 per group). A–C: Serum neutralizing antibody responses measured by PRNT on day 21 post-initial immunization, day 21 post-final immunization, and day 365 post-final immunization (n=8 per group). Data were analyzed using the Mann-Whitney test. D–F: Serum cross-neutralizing antibody responses against DENV2, DENV3, and DENV4 measured by PRNT on day 365 post-final immunization (n=8 per group). Data were analyzed using the Mann-Whitney test. ns: Not significant; *: P<0.05; **: P<0.01; ***: P<0.001; ****: P<0.0001. WT: Wild-type, DNSP: Dengue non-secreting particle.

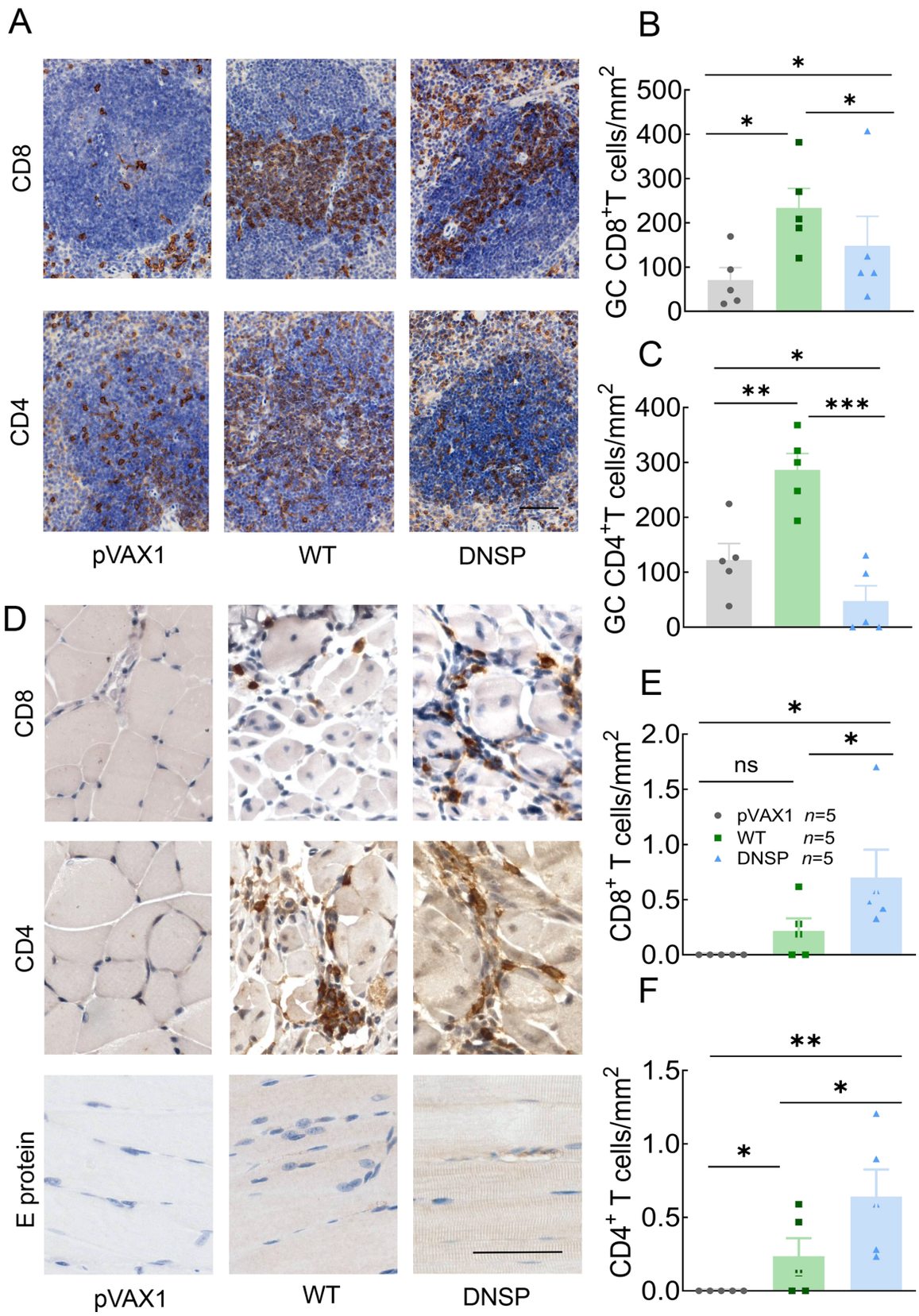

Figure 3 Cellular immune responses elicited by pVAX1-DENV1 DNA vaccine

Spleen and muscle tissues were collected 3 weeks after final immunization, and immunohistochemical staining was performed to assess $CD4^+$ and $CD8^+$ T cell distribution and abundance. A: Representative immunohistochemical images of spleen sections (n=5). Scale bar, 60 μm. B–C: Quantification of $CD4^+$ and $CD8^+$ T cells per field of view in splenic germinal centers (n=5). Statistical analysis was performed using the Mann-Whitney test. D: Representative immunohistochemical images of muscle tissue from the injection site (n=5). Scale bar, 60 μm. E–F: Quantification of $CD4^+$ and $CD8^+$ T cells per field of view in muscle tissue from the injection site (n=5). Statistical analysis was performed using the Mann-Whitney test. ns: Not significant; *: P<0.05; **: P<0.01; ***: P<0.001; ****: P<0.0001. GC: Germinal center, WT: Wild-type, DNSP: Dengue non-secreting particle.

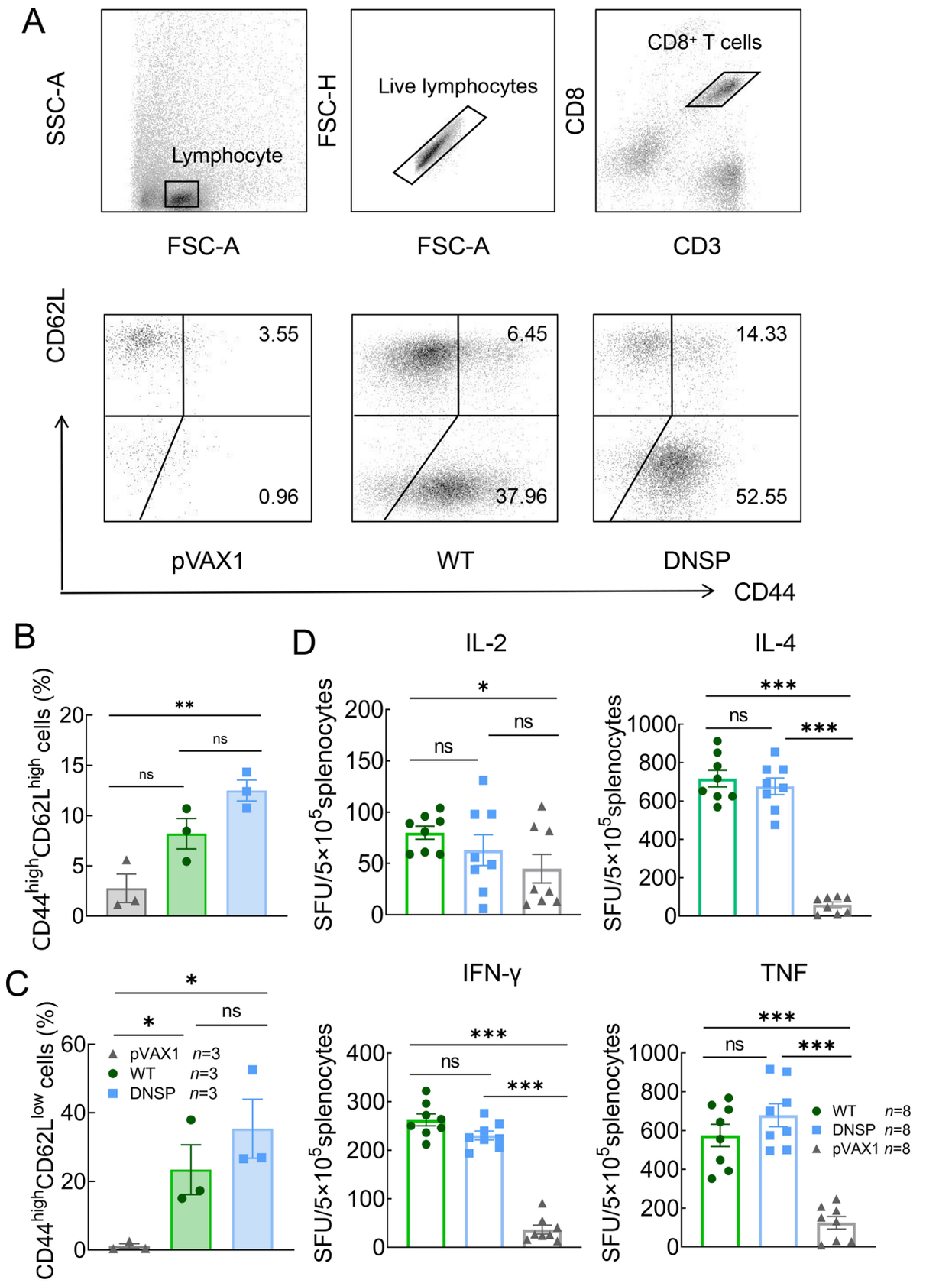

Figure 4 Memory T cell immunity and cytokine profiles elicited by pVAX1-DENV1 DNA vaccine

A: Spleens were collected 3 weeks after final immunization and subjected to flow cytometry to evaluate activation of antigen-specific $CD8^+$ $CD44^{high}$ memory T cells (n=3). B–C: Proportions of central memory T cells ($CD44^{high}$ $CD62L^{high}$) and effector memory T cells ($CD44^{high}$ $CD62L^{low}$). Values are expressed as mean (%)±SEM of the indicated cell population. Statistical analysis was performed using the Mann-Whitney test. D: Spleen cells were collected 3 weeks after final immunization and stimulated with full-length DENV1 protein to assess cytokine (IL-2, IL-4, IFN-γ, TNF) secretion (n=8). Results are presented as spot-forming units (SFU) per 5×10^5 splenocytes. Statistical analysis was performed using Student's t-test. ns: Not significant; *: P<0.05; **: P<0.01; ***: P<0.001; ****: P<0.0001. WT: Wild-type, DNSP: Dengue non-secreting particle.

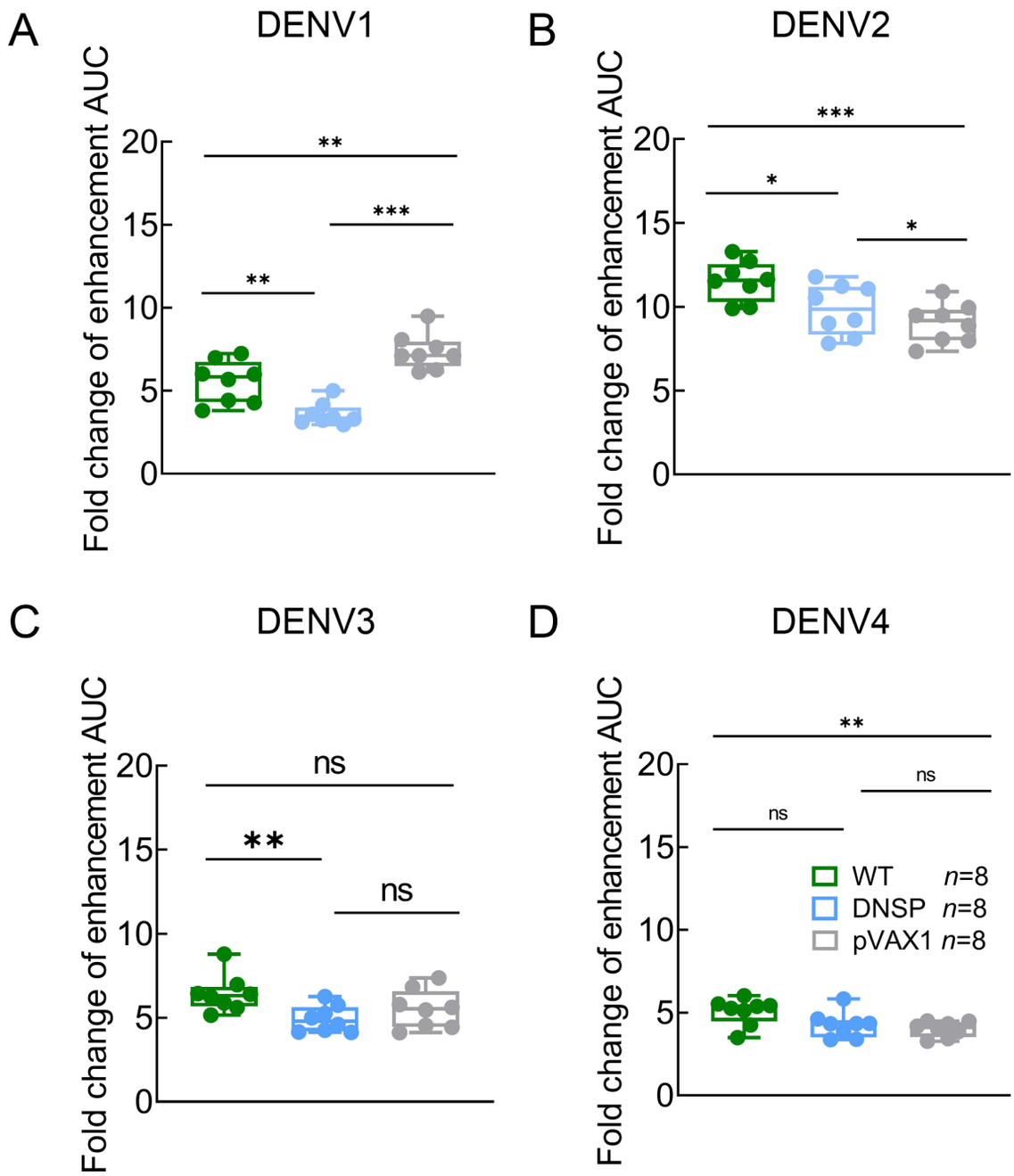

Figure 5 pVAX1-DNSP vaccine reduced enhancement of heterotypic DENV infection in K562 cells

Mouse serum collected 1 year post-immunization was co-incubated with DENV and then used to infect K562 cells. The proportion of infected cells was quantified, and the area under the curve (AUC) was calculated from the fitted curve of positive-cell ratios across serum dilutions relative to the detection baseline, representing serum ADE. A–D: ADE activity against DENV1, DENV2, DENV3, and DENV4, respectively. Statistical analysis was performed using the Mann-Whitney test (n=8). ns: Not significant; *: P<0.05; **: P<0.01; ***: P<0.001; ****: P<0.0001. AUC: Area under the curve, WT: Wild-type, DNSP: Dengue non-secreting particle.

DNSP, pVAX1-WT, or pVAX1-control and boosted according to the schedule described above. Three weeks after the final immunization, mice were challenged with 1×10^3 PFU of DENV1 Hawaii strain (GenBank ID: EU848545). In the short-term infection experiments, mice vaccinated with either pVAX1-DNSP or pVAX1-WT showed no significant body-weight loss or visible disease symptoms during the observation period. In contrast, the pVAX1-control group exhibited more than 25% body-weight loss between days 11 and 12 and developed overt clinical signs from days 7 to 18 (Figure 6A, B). Both vaccine groups were fully protected against DENV1-induced mortality, whereas the pVAX1-control group showed 22% mortality (Figure 6C), demonstrating effective short-term protection after pVAX1-DNSP immunization.

Long-term protection was evaluated by challenging mice 1 year after the final immunization using the same DENV1 challenge dose. Compared with pVAX1-WT-vaccinated mice, pVAX1-DNSP-vaccinated mice showed mild body-weight loss followed by gradual recovery. Clinical signs were more apparent in the pVAX1-DNSP group from days 3 to 18 but did not progress and resolved after day 18. In contrast, all mice in the pVAX1-control group died before day 24 (Figure 6D–F). These results demonstrate that both pVAX1-DNSP and pVAX1-WT provided complete protection against lethal DENV1 challenge at 3 weeks and 1 year post-immunization,

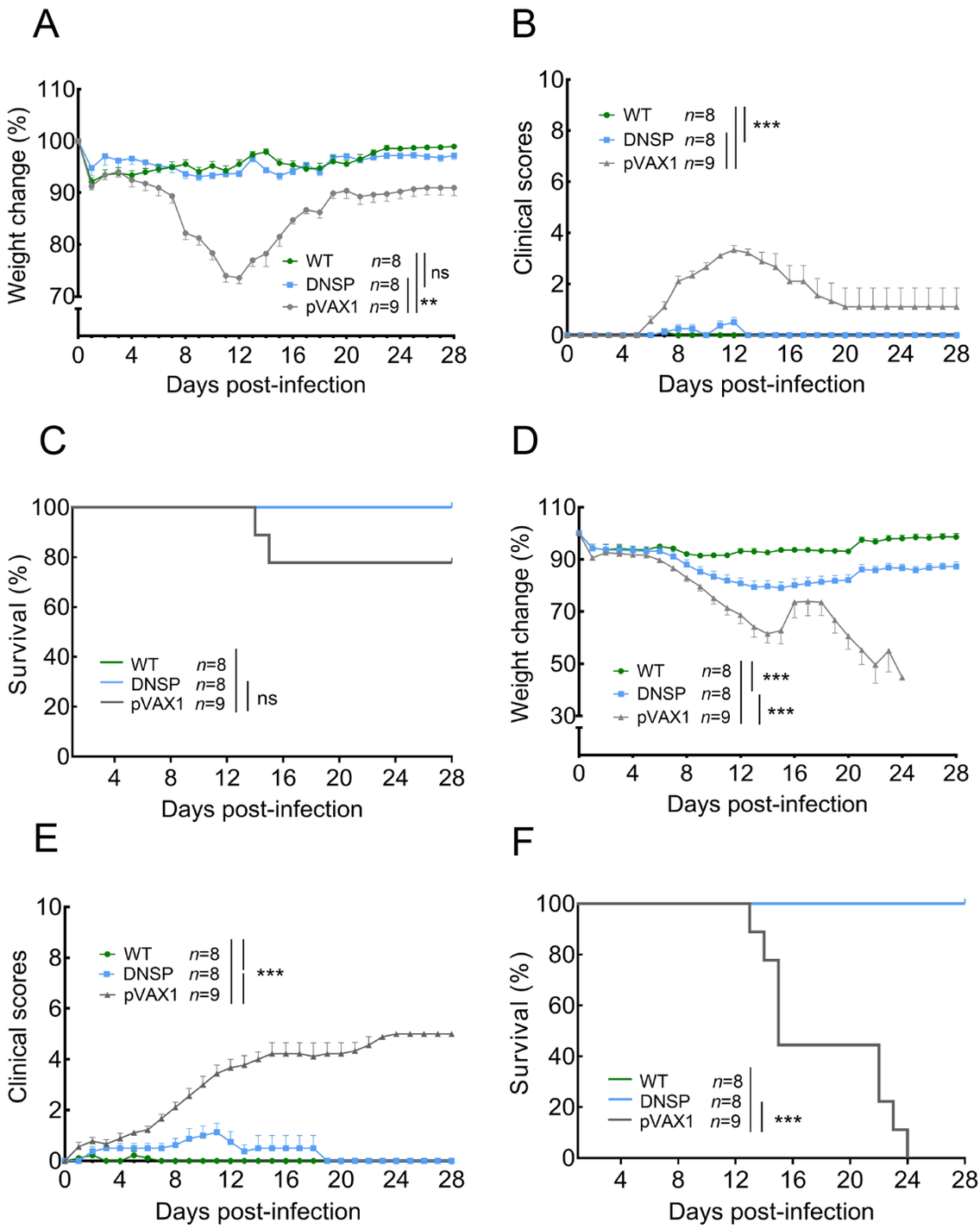

Figure 6 pVAX1-DNSP induces durable protective immunity

BALB/c mice received three doses of WT, DNSP, or pVAX1. At 3 weeks and 1 year after final immunization, mice were challenged with 1×10^3 PFU of DENV1. A–C: Body-weight change, clinical score, and survival after short-term DENV1 challenge (n=8–9). Body-weight change and clinical scores were analyzed by pairwise comparisons using the Mann-Whitney test. Survival was analyzed using the log-rank test followed by Bonferroni correction. D–F: Body-weight change, clinical score, and survival after long-term DENV1 challenge (n=8–9). Body-weight change and clinical scores were analyzed by pairwise comparisons using the Mann-Whitney test. Survival was analyzed using the log-rank test followed by Bonferroni correction. ns: Not significant; **: P<0.01; ***: P<0.001; ****: P<0.0001. WT: Wild-type, DNSP: Dengue non-secreting particle.

supporting durable protective efficacy against DENV1.

pVAX1-DNSP protects A6 mice against DENV2 infection

Given that both vaccine constructs conferred complete protection against lethal DENV1 infection, heterotypic protection and ADE-associated disease risk were further evaluated in A6 mice. Immune serum collected 3 weeks after the final immunization was incubated with DENV2 for 1 h and then administered to A6 mice. After DENV2 challenge, mice receiving serum from the pVAX1-DNSP group developed milder disease symptoms than those receiving serum from the pVAX1-WT group (Figure 7A–C). The pVAX1-DNSP group showed 100% survival, exceeding the survival rates observed in both the pVAX1-WT (77.8%) and empty-vector (77.8%) groups, indicating stronger protection under heterotypic challenge conditions. Whole-blood samples collected at 1 and

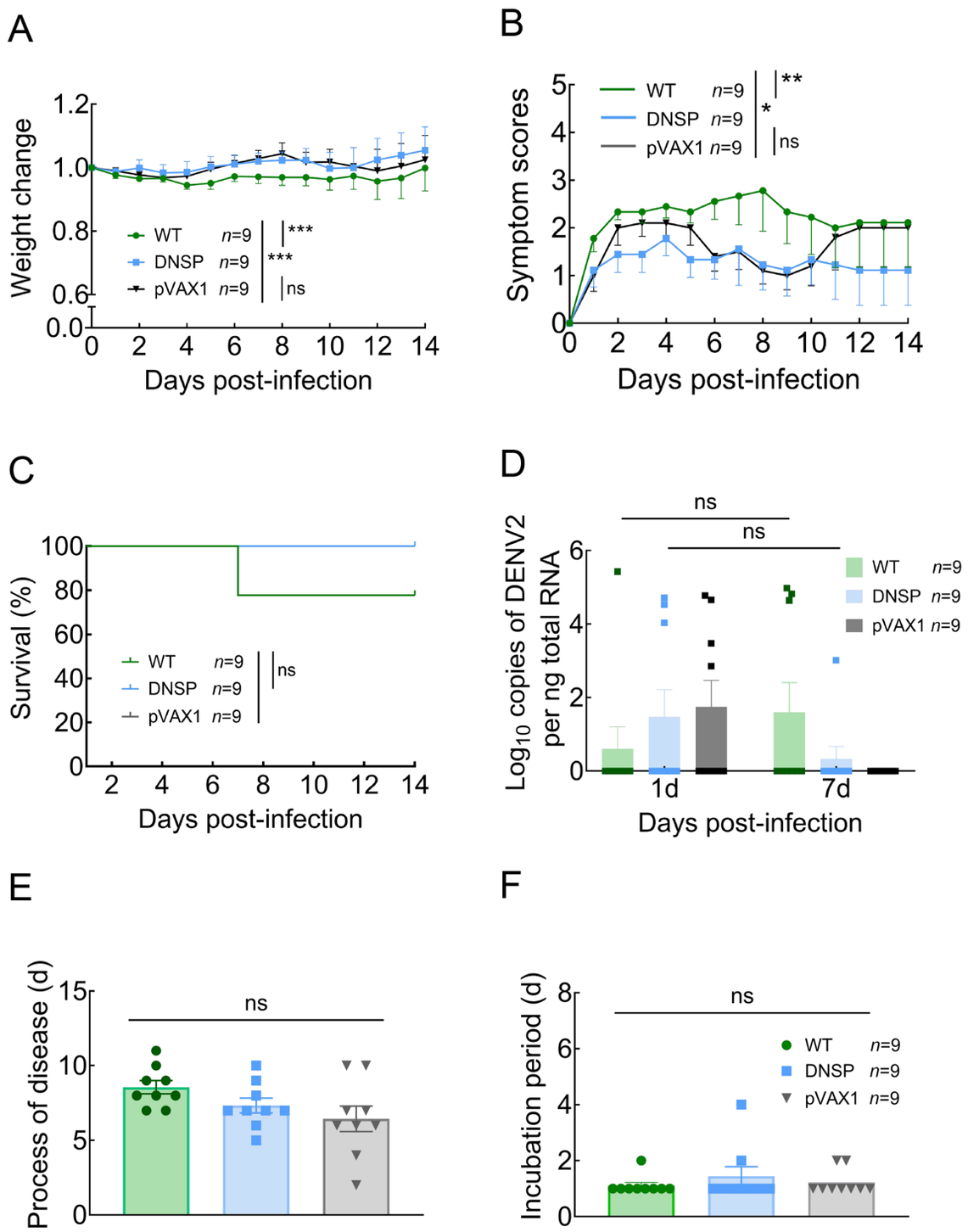

Figure 7 Serum from pVAX1-DNSP-immunized mice confers protection against DENV2 in A6 mice

BALB/c mice received three doses of WT, DNSP, or pVAX1. Three weeks after the final immunization, serum was collected, co-incubated with DENV2 for 1 h, and transferred into A6 mice. A–C: Body-weight change, clinical score, and survival after DENV2 challenge (n=9). Body-weight change and clinical scores were analyzed using the Mann-Whitney test. Survival was analyzed using the log-rank test. D: Serum collected at days 1 and 7 post-infection was used to quantify viral load (n=9). Viral loads were analyzed using the Mann-Whitney test. E: Latency period (n=9). Statistical analysis was performed using the Mann-Whitney test. F: Disease progression (n=9). Data were analyzed using the Mann-Whitney test. ns: Not significant; *: P<0.05; **: P<0.01; ***: P<0.001; ****: P<0.0001. WT: Wild-type, DNSP: Dengue non-secreting particle.

7 days post-infection (dpi) were used to quantify viral loads. Viral RNA levels increased over time in the pVAX1-WT group, whereas viral loads gradually decreased in the pVAX1-DNSP group (Figure 7D). Analysis of disease latency and progression showed no significant differences between the pVAX1-DNSP group and the other two groups (Figure 7E, F). These findings indicate that pVAX1-DNSP immune serum reduced DENV2 disease severity and improved survival in A6 mice, without evidence of enhanced disease after heterotypic DENV exposure.

DISCUSSION

Safe and durable DENV vaccination remains an urgent global public health challenge, largely because protection must

extend across four antigenically distinct DENV serotypes without increasing disease risk in individuals with limited or no prior DENV exposure (O'Driscoll et al., 2023; Wu et al., 2022). ADE is central to this challenge because subneutralizing or imbalanced antibody responses can facilitate FcγR-mediated infection, thereby compromising DENV vaccine safety and efficacy (Dejnirattisai et al., 2010). Multiple DENV vaccine platforms have therefore been developed, including live-attenuated, recombinant subunit, and mRNA-based approaches, with two vaccines receiving regulatory approval in different jurisdictions. Dengvaxia (CYD-TDV), developed by Sanofi Pasteur (Capeding et al., 2014; Hadinegoro et al., 2015; Henein et al., 2021; Sridhar et al., 2018; Villar et al., 2015), is a tetravalent chimeric vaccine based on the yellow fever vaccine YF17D backbone and has been approved for individuals aged 9–45 years with documented previous dengue infection. Qdenga (TAK003), developed by Takeda, is also a tetravalent chimeric vaccine, but it uses an attenuated DENV2 backbone (Biswal et al., 2019, 2020; López-Medina et al., 2022; Osorio et al., 2016; Rivera et al., 2022; Tricou et al., 2020). TAK003 received approval in Indonesia for individuals aged 9–45 years in August 2022 and in the European Union for individuals aged 4 years and older in December 2022. Additional candidates are advancing clinically. The US National Institutes of Health (NIH)-developed tetravalent live-attenuated TV003/TV005 vaccine has also shown promising progress. (Durbin, 2020; Kirkpatrick et al., 2015, 2016; Pierce et al., 2024; Walsh et al., 2024; Whitehead, 2016) The latest data indicate that TV003 vaccine shows no safety issues observed during the 5-year follow-up period. (Kallas et al., 2026) Phase III data for the Butantan-DV vaccine, developed by the Butantan Institute in Brazil, demonstrated strong protection against DENV1 and DENV2 (Kallás et al., 2024; Kallas et al., 2020). Despite these advances, long-term efficacy, serotype balance, and safety in populations with diverse baseline immune status remain unresolved. Ongoing research into alternative prevention and treatment strategies is therefore essential to complement existing vaccine efforts (Halstead, 2016).

Previous studies have identified key host trafficking factors, including Arf4, Arf5, and KDELRs, as important regulators of DENV secretion (Kudelko et al., 2012; Kuhn et al., 2002; Li et al., 2015). KDELRs cycle between the ER and Golgi apparatus and have been proposed to interact with DENV prM, thereby facilitating viral transport through the early secretory pathway. (Lewis & Pelham, 1992; Raykhel et al., 2007; Volpicelli-Daley et al., 2005). Mapping of the prM-KDELR interaction further identified residues 2, 19, and 21 of prM as critical determinants of KDELR binding. Substitution of these residues preserved production of DENV subviral particles but prevented their extracellular release, generating secretion-deficient particles with a distinct antigen-distribution profile. These secretion-deficient subviral particles are therefore ideal candidates for inducing low humoral immunity and high cellular immunity. Accordingly, pVAX1-based DNA vaccines were generated to express either full-length prM-E proteins (WT) or secretion-deficient prM-E proteins (DNSP). The two constructs produced clearly different humoral immune profiles: DNSP induced significantly lower DENV-specific IgG levels than WT at early post-immunization time points. The mechanism underlying this difference remains unresolved, but it may be related to altered antigen trafficking and subsequent differences in immune processing between intracellularly retained DNSP antigens and secreted WT antigens. At later time points, neutralizing and cross-reactive antibody responses induced by DNSP against DENV1, DENV3, and DENV4 were comparable to those observed in the pVAX1-control group. This background reactivity may be related to nonspecific immunostimulatory effects of the empty vector plasmid (pVAX1) in mice, which may trigger the production of a small amount of IgG with weak binding capacity to DENV1 antigen (Sawamura et al., 2005; Wu-Chuang et al., 2024). Despite this background signal, DNSP and WT showed marked differences in antibody production.

Secretion-deficient particles retained within the cell are thought to enter endogenous antigen-processing pathways because impaired extracellular release increases intracellular proteasomal degradation (MacNabb et al., 2022). The resulting short peptides can be transported into the ER through transporter associated with antigen processing (TAP), where they bind to MHC class I molecules and are subsequently presented on the cell surface as peptide-MHC class I complexes. This pathway enables recognition by $CD8^+$ T cells and promotes expansion and differentiation into effector CTLs, which eliminate virus-infected cells. In contrast, limited extracellular release reduces antigen availability for uptake by APCs through phagocytosis or endocytosis. Restricted entry into the exogenous antigen-processing pathway may reduce lysosomal degradation, MHC class II loading, $CD4^+$ T cell activation, and downstream B cell activation, thereby attenuating antibody production (Blander, 2023).

Consistent with this model, DNSP immunization induced substantial $CD8^+$ T cell infiltration at the muscle injection site 3 weeks after the final immunization. The magnitude of $CD8^+$ T cell activation was comparable to that induced by WT, suggesting that the secretion-deficient vaccine can elicit robust $CD8^+$ T cell-mediated immunity. In splenic germinal centers, DNSP also generated $CD8^+$ T cell numbers similar to those induced by WT but was associated with significantly fewer $CD4^+$ T cells than the WT construct. These findings suggest that secretion-deficient prM-E expression redirects the immune response toward $CD8^+$ T cell activity while partially limiting the helper pathways that support humoral immunity. Functional analysis further showed that splenic CTLs from DNSP-immunized mice mediated dose-dependent target-cell killing *in vitro* at levels comparable to those induced by WT. DENV1-specific cellular immune response assays also demonstrated that DNSP promoted cellular immunity and increased secretion of Th1-associated cytokines. Together with the DENV1 challenge data, these results indicate that DNSP provided durable protection despite reduced antibody induction, supporting an important contribution of cellular immunity to DNSP-mediated protection. Nevertheless, these experiments did not define the antigen-processing pathway responsible for DNSP-induced $CD8^+$ T cell cytotoxicity. Although DNSP vaccination increased antigen-specific CTL activity, direct evidence that DNSP-derived peptides are processed and presented through the MHC class I pathway remains lacking. Future studies using MHC-I tetramer staining and antigen-specific CD8+ T cell tracking will be needed to clarify this mechanism.

Serum collected 1 year after immunization was co-incubated with heterologous DENV and then applied to K562 cells to evaluate ADE activity. DNSP immune serum did not increase DENV2, DENV3, or DENV4 infection above the pVAX1-control level, supporting the potential of this secretion-deficient construct to reduce ADE risk after heterotypic DENV

exposure. In the DENV1 infection assay, infection efficiency across the four serum dilutions (1:10 to 1:10 000) was consistently higher in the pVAX1-control group than in the WT and DNSP groups (Supplementary Figure S2). This background effect may reflect non-specific immune activation by the plasmid backbone, including CpG motif-mediated TLR9 signaling (Klinman et al., 1997), naturally occurring or cross-reactive antibodies in mouse serum (Hadzhieva et al., 2016), or low-affinity antibody production after prolonged immune stimulation (Sprumont et al., 2023). Importantly, the WT and DNSP constructs both encode DENV1 prM-E-derived immunogens, and serum from mice in these groups contained DENV1-specific neutralizing components. Across all four dilution conditions, the proportion of infected cells was significantly higher in the WT group than in the DNSP group. In addition, in heterotypic infection assays using DENV2, DENV3, and DENV4, infection AUC values were significantly higher in the WT group than in the DNSP group (P<0.05). These results suggest that the signal observed in the pVAX1-control group most likely represented experimental background, whereas WT vaccination generated a higher ADE-associated infection profile. In contrast, DNSP reduced ADE-associated infection profiles across all tested serum dilutions and viral serotypes.

Several limitations should nevertheless be considered. The K562 assay provides a useful first-line platform for initial ADE risk screening but does not fully recapitulate human DENV pathogenesis. Future research should evaluate ADE risk associated with DNSP using primary human monocytes, macrophages, and relevant humanized animal models. In the DENV2 infection model, the DNSP group exhibited milder clinical signs, higher survival, and faster viral clearance from whole blood compared to the WT group. These findings indicate that the DNSP vaccine elicits robust cellular immunity, particularly Th1-biased responses, while limiting antibody production relative to WT vaccination. This immune profile supports DNSP as a promising T cell-targeted DENV vaccine candidate for further development.

Several T-cell-targeted DENV vaccine platforms remain under preclinical development, and the secretion-deficient DNA vaccine described here both overlaps with and diverges from these approaches in the pattern of cellular immunity induced. Similar to DENV mRNA vaccines targeting E-DIII, our strategy incorporated the E protein as the primary antigenic component (Alameh et al., 2021; He et al., 2022). However, reported immunodominant epitopes in E and NS1, including the E40 and N67 peptides, show particularly strong capacity for T cell induction (Pinto et al., 2019) and may provide rational targets for further antigen optimization. Adenovirus-vectored flavivirus vaccines have also been shown to generate strong Th1-biased cellular immunity (Bullard et al., 2018), aligning with the $CD8^+$ T cell-dominant response observed in the current study. Additionally, studies examining cross-reactive T cells against heterologous flaviviruses suggest that a multi-target DNA vaccine design based on both E and NS proteins may provide broader protection than traditional E-only strategies (Subramaniam et al., 2020). Collectively, these findings underscore the critical role of T cell immunity in DENV vaccine research. The observed differences in immunogenicity across vaccine platforms may offer novel avenues for combination immunization strategies, aimed at balancing the magnitude and durability of the immune response.

Overcoming ADE remains one of the central problems in DENV vaccine development. Recent studies have advanced both mechanistic understanding and experimental strategies for reducing this risk. Wang et al. (2023) established an ADE model by co-incubating anti-DENV2 prM serum with DENV3 before infection of A129 mice. The ADE group developed more severe hepatic, intestinal, and pulmonary injury after DENV3 infection, accompanied by significantly higher TGF-β and TNF-α levels than those in uninfected controls, confirming successful model establishment (Wang et al., 2023). Modhiran et al. (2021) developed a broadly protective antibody targeting NS1 and evaluated blockade of NS1 activity across multiple flaviviruses *in vitro* and *in vivo*. Despite differences in cytotoxicity among NS1 proteins from distinct flaviviruses, this antibody significantly reduced viral load and circulating NS1 levels in lethal animal models (Modhiran et al., 2021). In another approach, Wang et al. (2020) generated TetraM-E, a tetrameric DNA vaccine incorporating prM-E proteins from all four DENV serotypes as immunogens. Heterologous DENV antigen exposure after immunization increased Th1/Th2 cytokine production, and long-term evaluation showed that tetravalent DENV antibody responses remained detectable 30 weeks post-immunization, with protection against all four DENV serotypes (Wang et al., 2020). Together, these studies substantially advance solutions to key challenges in DENV vaccine development, thereby providing a valuable reference for subsequent research.

In summary, this study showed that DNSP immunization induced low antibody responses while preserving robust cellular immunity. pVAX1-DNSP was sufficient to confer durable protection against lethal DENV1 challenge and improved serum-mediated protection against DENV2 infection in two experimental models. However, because *in vivo* challenge experiments with DENV3 and DENV4 were not performed, the cross-protective efficacy of DNSP against these serotypes remains unresolved and represents an important limitation. Nevertheless, our experimental findings provide valuable insights for future investigations and underscore the critical role of cellular immunity in protecting against DENV infection. This strategy provides a framework for developing safer next-generation DENV vaccines with improved control of enhancement risk.

SUPPLEMENTARY DATA

Supplementary data to this article can be found online.

COMPETING INTERESTS

The authors declare that they have no competing interests.

AUTHORS' CONTRIBUTIONS

C.Z. and K.H.F. performed the experiments and analyzed the data. Y.X.L., C.Y.Z., and K.Q.L. performed animal experiments. H.C. and D.Y.F. helped maintain cells and viruses. J.A,, P.G.W., and N.G. conceived the project, analyzed the data, and wrote and reviewed the manuscript. J.A. coordinated the whole study. The authors declare that they have no known competing financial interests or personal relationships that could have appeared to influence the work reported in this paper. All authors read and approved the final version of the manuscript.

REFERENCES

Aggarwal C, Ahmed H, Sharma P, et al. 2024. Severe disease during both primary and secondary dengue virus infections in pediatric populations. *Nature Medicine*, **30**(3): 670–674.

Alameh MG, Tombácz I, Bettini E, et al. 2021. Lipid nanoparticles enhance the efficacy of mRNA and protein subunit vaccines by inducing robust T

follicular helper cell and humoral responses. *Immunity*, **54**(12): 2877–2892. e7.

Bhatt S, Gething PW, Brady OJ, et al. 2013. The global distribution and burden of dengue. *Nature*, **496**(7446): 504–507.

Biswal S, Borja-Tabora C, Martinez Vargas L, et al. 2020. Efficacy of a tetravalent dengue vaccine in healthy children aged 4–16 years: a randomised, placebo-controlled, phase 3 trial. *The Lancet*, **395**(10234): 1423–1433.

Biswal S, Reynales H, Saez-Llorens X, et al. 2019. Efficacy of a tetravalent dengue vaccine in healthy children and adolescents. *The New England Journal of Medicine*, **381**(21): 2009–2019.

Blander JM. 2023. Different routes of MHC-I delivery to phagosomes and their consequences to CD8 T cell immunity. *Seminars in Immunology*, **66**: 101713.

Bullard BL, Corder BN, Gorman MJ, et al. 2018. Efficacy of a T cell-biased adenovirus vector as a Zika virus vaccine. *Scientific Reports*, **8**(1): 18017.

Capeding MR, Tran NH, Hadinegoro SRS, et al. 2014. Clinical efficacy and safety of a novel tetravalent dengue vaccine in healthy children in Asia: a phase 3, randomised, observer-masked, placebo-controlled trial. *The Lancet*, **384**(9951): 1358–1365.

Copaja-Corzo C, Flores-Cohaila J, Tapia-Sequeiros G, et al. 2024. Risk factors associated with dengue complications and death: a cohort study in Peru. *PLoS One*, **19**(6): e0305689.

Dejnirattisai W, Jumnainsong A, Onsirisakul N, et al. 2010. Cross-reacting antibodies enhance dengue virus infection in humans. *Science*, **328**(5979): 745–748.

Durbin AP. 2020. Historical discourse on the development of the live attenuated tetravalent dengue vaccine candidate TV003/TV005. *Current Opinion in Virology*, **43**: 79–87.

Guirakhoo F, Arroyo J, Pugachev KV, et al. 2001. Construction, safety, and immunogenicity in nonhuman primates of a chimeric yellow fever-dengue virus tetravalent vaccine. *Journal of Virology*, **75**(16): 7290–7304.

Guo CC, Zhou ZX, Wen ZH, et al. 2017. Global epidemiology of dengue outbreaks in 1990–2015: a systematic review and meta-analysis. *Frontiers in Cellular and Infection Microbiology*, **7**: 317.

Hadinegoro SR, Arredondo-García JL, Capeding MR, et al. 2015. Efficacy and long-term safety of a dengue vaccine in regions of endemic disease. *The New England Journal of Medicine*, **373**(13): 1195–1206.

Hadzhieva M, Vassilev T, Bayry J, et al. 2016. Relationship between natural and heme-mediated antibody polyreactivity. *Biochemical and Biophysical Research Communications*, **472**(1): 281–286.

Halstead SB. 2016. Critique of world health organization recommendation of a dengue vaccine. *The Journal of Infectious Diseases*, **214**(12): 1793–1795.

Halstead SB, Crowe JE, Boraschi D, et al. 2014. Dengue antibody-dependent enhancement: knowns and unknowns. *Microbiology Spectrum*, **2**(6). doi: 10.1128/microbiolspec.aid-0022-2014.

He LH, Sun WQ, Yang LM, et al. 2022. A multiple-target mRNA-LNP vaccine induces protective immunity against experimental multi-serotype DENV in mice. *Virologica Sinica*, **37**(5): 746–757.

Henein S, Adams C, Bonaparte M, et al. 2021. Dengue vaccine breakthrough infections reveal properties of neutralizing antibodies linked to protection. *The Journal of Clinical Investigation*, **131**(13): e147066.

Kallás EG, Cintra MAT, Moreira JA, et al. 2024. Live, attenuated, tetravalent Butantan-dengue vaccine in children and adults. *The New England Journal of Medicine*, **390**(5): 397–408.

Kallas EG, Precioso AR, Palacios R, et al. 2020. Safety and immunogenicity of the tetravalent, live-attenuated dengue vaccine Butantan-DV in adults in Brazil: a two-step, double-blind, randomised placebo-controlled phase 2 trial. *The Lancet Infectious Diseases*, **20**(7): 839–850.

Kariyawasam R, Lachman M, Mansuri S, et al. 2023. A dengue vaccine whirlwind update. *Therapeutic Advances in Infectious Disease*, **10**: 20499361231167274.

Kayesh MEH, Khalil I, Kohara M, et al. 2023. Increasing dengue burden and severe dengue risk in Bangladesh: an overview. *Tropical Medicine and Infectious Disease*, **8**(1): 32.

Kirkpatrick BD, Durbin AP, Pierce KK, et al. 2015. Robust and balanced immune responses to all 4 dengue virus serotypes following administration of a single dose of a live attenuated tetravalent dengue vaccine to healthy, flavivirus-naive adults. *The Journal of Infectious Diseases*, **212**(5): 702–710.

Kirkpatrick BD, Whitehead SS, Pierce KK, et al. 2016. The live attenuated dengue vaccine TV003 elicits complete protection against dengue in a human challenge model. *Science Translational Medicine*, **8**(330): 330ra36.

Klinman DM, Yamshchikov G, Ishigatsubo Y. 1997. Contribution of CpG motifs to the immunogenicity of DNA vaccines. *The Journal of Immunology*, **158**(8): 3635–3639.

Kudelko M, Brault JB, Kwok K, et al. 2012. Class II ADP-ribosylation factors are required for efficient secretion of dengue viruses. *Journal of Biological Chemistry*, **287**(1): 767–777.

Kuhn RJ, Zhang W, Rossmann MG, et al. 2002. Structure of dengue virus: implications for flavivirus organization, maturation, and fusion. *Cell*, **108**(5): 717–725.

Lee SY, Shih HI, Lo WC, et al. 2024. Discrepancies in dengue burden estimates: a comparative analysis of reported cases and global burden of disease study, 2010–2019. *Journal of Travel Medicine*, **31**(4): taae069.

Lewis MJ, Pelham HRB. 1992. Sequence of a second human KDEL receptor. *Journal of Molecular Biology*, **226**(4): 913–916.

Li MY, Grandadam M, Kwok K, et al. 2015. KDEL receptors assist dengue virus exit from the endoplasmic reticulum. *Cell Reports*, **10**(9): 1496–1507.

López-Medina E, Biswal S, Saez-Llorens X, et al. 2022. Efficacy of a dengue vaccine candidate (TAK-003) in healthy children and adolescents 2 years after vaccination. *The Journal of Infectious Diseases*, **225**(9): 1521–1532.

MacNabb BW, Chen XF, Tumuluru S, et al. 2022. Dendritic cells can prime anti-tumor $CD8^+$ T cell responses through major histocompatibility complex cross-dressing. *Immunity*, **55**(6): 982–997. e8.

Martinez DR, Metz SW, Baric RS. 2021. Dengue vaccines: the promise and pitfalls of antibody-mediated protection. *Cell Host & Microbe*, **29**(1): 13–22.

Modhiran N, Song H, Liu LD, et al. 2021. A broadly protective antibody that targets the flavivirus NS1 protein. *Science*, **371**(6525): 190–194.

O'Driscoll M, Buddhari D, Huang AT, et al. 2023. Maternally derived antibody titer dynamics and risk of hospitalized infant dengue disease. *Proceedings of the National Academy of Sciences of the United States of America*, **120**(41): e2308221120.

Osorio JE, Wallace D, Stinchcomb DT. 2016. A recombinant, chimeric tetravalent dengue vaccine candidate based on a dengue virus serotype 2 backbone. *Expert Review of Vaccines*, **15**(4): 497–508.

Paz-Bailey G, Adams LE, Deen J, et al. 2024. Dengue. *The Lancet*, **403**(10427): 667–682.

Pierce KK, Durbin AP, Walsh MCR, et al. 2024. TV005 dengue vaccine protects against dengue serotypes 2 and 3 in two controlled human infection studies. *The Journal of Clinical Investigation*, **134**(3): e173328.

Pinto PBA, Assis ML, Vallochi AL, et al. 2019. T cell responses induced by DNA vaccines based on the DENV2 E and NS1 proteins in mice: importance in protection and immunodominant epitope identification. *Frontiers in Immunology*, **10**: 1522.

Raykhel I, Alanen H, Salo K, et al. 2007. A molecular specificity code for the three mammalian KDEL receptors. *The Journal of Cell Biology*, **179**(6): 1193–1204.

Rivera L, Biswal S, Sáez-Llorens X, et al. 2022. Three-year efficacy and safety of Takeda's dengue vaccine candidate (TAK-003). *Clinical Infectious Diseases*, **75**(1): 107–117.

Sahak MN. 2020. Dengue fever as an emerging disease in Afghanistan:

epidemiology of the first reported cases. *International Journal of Infectious Diseases*, **99**: 23–27.

Santos-Peral A, Luppa F, Goresch S, et al. 2024. Prior flavivirus immunity skews the yellow fever vaccine response to cross-reactive antibodies with potential to enhance dengue virus infection. *Nature Communications*, **15**(1): 1696.

Sawamura D, Abe R, Goto M, et al. 2005. Direct injection of plasmid DNA into the skin induces dermatitis by activation of monocytes through toll-like receptor 9. *The Journal of Gene Medicine*, **7**(5): 664–671.

Shepard DS, Undurraga EA, Halasa YA, et al. 2016. The global economic burden of dengue: a systematic analysis. *The Lancet Infectious Diseases*, **16**(8): 935–941.

Sprumont A, Rodrigues A, McGowan SJ, et al. 2023. Germinal centers output clonally diverse plasma cell populations expressing high- and low-affinity antibodies. *Cell*, **186**(25): 5486–5499. e13.

Sridhar S, Luedtke A, Langevin E, et al. 2018. Effect of dengue serostatus on dengue vaccine safety and efficacy. *The New England Journal of Medicine*, **379**(4): 327–340.

Subramaniam KS, Lant S, Goodwin L, et al. 2020. Two is better than one: evidence for T-cell cross-protection between dengue and Zika and implications on vaccine design. *Frontiers in Immunology*, **11**: 517.

Thomas SJ, Yoon IK. 2019. A review of Dengvaxia®: development to deployment. *Human Vaccines & Immunotherapeutics*, **15**(10): 2295–2314.

Tian N, Zheng JX, Guo ZY, et al. 2022. Dengue incidence trends and its burden in major endemic regions from 1990 to 2019. *Tropical Medicine and Infectious Disease*, **7**(8): 180.

Tricou V, Sáez-Llorens X, Yu DL, et al. 2020. Safety and immunogenicity of a tetravalent dengue vaccine in children aged 2–17 years: a randomised, placebo-controlled, phase 2 trial. *The Lancet*, **395**(10234): 1434–1443.

Villar L, Dayan GH, Arredondo-García JL, et al. 2015. Efficacy of a tetravalent dengue vaccine in children in Latin America. *The New England Journal of Medicine*, **372**(2): 113–123.

Volpicelli-Daley LA, Li YW, Zhang CJ, et al. 2005. Isoform-selective effects of the depletion of ADP-ribosylation factors 1–5 on membrane traffic. *Molecular Biology of the Cell*, **16**(10): 4495–4508.

Vuong NL, Quyen NTH, Tien NTH, et al. 2024. Dengue viremia kinetics and effects on platelet count and clinical outcomes: an analysis of 2340 patients from Vietnam. *eLife*, **13**: RP92606.

Walsh MCR, Alam MS, Pierce KK, et al. 2024. Safety and durable immunogenicity of the TV005 tetravalent dengue vaccine, across serotypes and age groups, in dengue-endemic Bangladesh: a randomised, controlled trial. *The Lancet Infectious Diseases*, **24**(2): 150–160.

Wang H, Long MW, Zhang L, et al. 2023. Establishment of a non-lethal model of antibody-dependent enhancement of infection in A129 mice based on a non-mouse-adapted dengue virus strain. *Zoological Research*, **44**(5): 943–946.

Wang R, Yang FJ, Zheng XY, et al. 2020. Long-term protection against dengue viruses in mice conferred by a tetravalent DNA vaccine candidate. *Zoological Research*, **41**(1): 90–93.

Whitehead SS. 2016. Development of TV003/TV005, a single dose, highly immunogenic live attenuated dengue vaccine; what makes this vaccine different from the Sanofi-Pasteur CYD™ vaccine?. *Expert Review of Vaccines*, **15**(4): 509–517.

Wu TT, Wu ZD, Li YP. 2022. Dengue fever and dengue virus in the People's Republic of China. *Reviews in Medical Virology*, **32**(1): e2245.

Wu-Chuang A, Rojas A, Bernal C, et al. 2024. Influence of microbiota-driven natural antibodies on dengue transmission. *Frontiers in Immunology*, **15**: 1368599.

Yue YJ, Liu QY, Liu XB, et al. 2022. Dengue fever in mainland China, 2005–2020: a descriptive analysis of dengue cases and *Aedes* data. *International Journal of Environmental Research and Public Health*, **19**(7): 3910.

Kallas EG, Moreira JA, Patino EG, et al. 2026. Long-term efficacy and safety of the single-dose tetravalent Butantan dengue vaccine. *Nat Med*, **32**(4): 1393–1400.

Tan TY, Fibriansah G, Kostyuchenko VA, et al. 2020. Capsid protein structure in Zika virus reveals the flavivirus assembly process. *Nat Commun*, **11**(1): 895.